A Model for Surfactant Distribution in Latex Coatings

Venkata R. Gundabala, William B. Zimmerman, and Alexander F. Routh*

Department of Chemical and Process Engineering, University of Sheffield, Mappin Street, Sheffield, S1 3JD, U.K.

Received April 28, 2004. In Final Form: July 19, 2004

The presence of surfactants in dried latex films can adversely affect the adhesive, water-resistant, and gloss properties, so investigating the surfactant distribution in latex coatings is of prime industrial relevance. Here we present a model that predicts the distribution of surfactant in a latex coating during the solvent evaporation stage. The conservation equation for surfactant during solvent evaporation is solved in the limit of infinite particle Peclet numbers, a dimensionless quantity giving the measure of relative magnitudes of evaporative to diffusive fluxes. A parametric analysis using the model reveals that the surfactant adsorption isotherm is the determining physical parameter. The model always predicts surfactant excesses at the top surface and either excess or depletion at the bottom surface depending on the isotherm. Uniform distributions are predicted for low surfactant Peclet numbers. Attenuated total reflection Fourier transform infrared spectroscopic probes on film surfaces conform to the behavior predicted by the model.

Introduction

Water-based latex coatings are fast replacing the traditional solvent-based coatings due to the polluting effects of the latter.[1] Latex coatings are dispersions of polymer particles in a suspending medium, usually water. Their use in most applications is based on the formation of a continuous film during drying. Latex film formation is generally considered to be a three-stage process involving the transition of a stable dispersion into a continuous clear mechanically integral polymeric film.[2]

Surfactants play a crucial role in latex dispersion synthesis and film formation. They provide colloidal stability to latex dispersions during synthesis. They affect particle ordering,[3,4] particle deformation,[5] and polymer chain interdiffusion.[6,7] The presence of surfactants is also known to adversely affect the adhesive,[8] water-resistant,[9] and gloss properties of dried latex films. Surfactant migration toward the film−substrate interface, which may be a result of several factors, can cause adhesive failure.[8] Surfactant excess at the film surface results in poor gloss and tackiness of the surface.[2] Excess surfactant presence during film formation can also result in improper particle packing and deformation, thereby leading to incomplete film formation and the presence of voids.[2] This causes high water uptake in the films, thus affecting the water-resistant properties. The need to minimize the detrimental affects of surfactant presence in dried latex films has propelled an intensive research effort in recent years.

Research into surfactant distribution in latex films was pioneered by Wagner and Fischer[10] as early as 1936. Since then, several researchers have dealt with the surfactant distribution problem. Attenuated total reflectance (ATR) and step-scan photoacoustic Fourier transform infrared (FTIR) spectroscopy, atomic force microscopy (AFM), infrared microscopy, Rutherford backscattering spectroscopy (RBS), and Raman spectroscopy have all been widely employed to study surfactant distribution at latex surfaces and film−substrate interfaces for various surfactant−latex systems.

The first major effort to study surfactant distribution and provide a mechanism for surfactant transport was made by Zhao et al.[11] Though their work was limited to anionic surfactants, they provided a general interpretation to enrichment: Tendency of surfactant to reduce interfacial energy drives it initially to the two interfaces; Water flux carries nonadsorbed surfactant to the film−air interface; Surfactant−polymer incompatibility provides the driving force for long time migration toward interfaces. Later works by other researchers have all invoked arguments similar to these to explain surfactant distribution. The fact that the surfactant tendency to reduce interfacial energy is one of the driving forces for surfactant transport toward the interfaces was confirmed by Evanson et al.[12] Their ATR-FTIR studies showed that other conditions remaining the same, substrates with lower surface energies induced greater surfactant enrichments toward the substrate side. This was due to the surfactant transport toward the substrate side to lower the interfacial surface tension that existed between the polymer latex and the substrate. Though researchers[11,12] have invoked substrate influence to account for surfactant excesses observed at the substrate side, the exact properties of the substrate which are responsible for influencing surfactant distribution are yet to be thoroughly studied.

FTIR spectroscopy was found to be a very useful tool in probing latex film surfaces. Groups involving Evanson et al. and Zhao et al. have used ATR-FTIR spectroscopy to study surfactant distribution in core−shell latex films, latex blends, and latex copolymers. Corroborating Zhao et al.'s[11] interpretation of enrichment at interfaces,

* To whom correspondence may be addressed. E-mail: a.routh@sheffield.ac.uk.

(1) Winnik, M. A. *Curr. Opinion Colloid Interface Sci.* **1997**, *2*, 52.
(2) Keddie, J. L. *Mater. Sci. Eng.* **1997**, *21*, 101.
(3) Issacs, P. K. *J. Macromol. Chem.* **1966**, *1* (1), 163.
(4) Okubo, M.; Takeya, T.; Tsutsumi, Y.; Kadooka, T.; Matsumoto, T. *J. Polym. Sci.: Polym. Chem.* **1981**, *19*, 1.
(5) Eckersley, S. T.; Rudin, A. *J. Appl. Polym. Sci.* **1993**, *48*, 1369.
(6) Farinha, J. P. S.; G Martinho, J. M.; Kawaguchi, S.; Yekta, A.; Winnik, M. A. *J. Phys. Chem.* **1996**, *100*, 12552.
(7) Kawaguchi, S.; Odrobina, E.; Winnik, M. A. *Macromol. Rapid Commun.* **1995**, *16*, 861.
(8) Zhao, C. L.; Holl, Y.; Pith, T.; Lambla, M. *Br. Polym. J.* **1989**, *21*, 155.
(9) Mulvihill, J.; Toussaint, A.; De Wilde, M. *Prog. Org. Coat.* **1997**, *30*, 127.
(10) Wagner, H.; Fischer, G. *Kolloid-A.* **1936**, *77*, 12.
(11) Zhao, C. L.; Dobler, F.; Pith, T.; Holl, Y.; Lambla, M. *J. Colloid Interface Sci.* **1989**, *128* (2), 437.
(12) Evanson, K. W. Urban, M. W. *J. Appl. Polym. Sci.* **1991**, *42*, 2309.

10.1021/la048939b CCC: $27.50
Published on Web 09/01/2004

Evanson et al.[13] showed that better compatibility between nonionic surfactants and EA/MMA latex resulted in less exudation toward interfaces. The issue of surfactant−polymer compatibility influence on surfactant stratification was also addressed by Zhao et al.[14] They invoked the lower compatibility between styrene and the anionic surfactant (sodium dioctylsulfosuccinate (SDOSS)) to account for the surfactant stratifications seen in styrene/*n*-butyl acrylate copolymer latex films. Zhao et al.'s work also stressed the utility of step-scan photoacoustic FTIR spectroscopy for depth profiling. In subsequent work, Zhao et al.[15] showed that exudation can also be controlled by adjusting the adsorption isotherm of the latex−surfactant system.

Kientz and Holl[16] studied the evolution of distribution of anionic, cationic, and nonionic surfactants in poly(2-ethylhexyl methacrylate) latex films. These systems belong to the incompatible surfactant−latex group and hence there is little or no dissolution of the surfactant into the polymer. They found that surfactant distribution is well established during the water evaporation stage and only morphological changes occur thereafter. This view was later corroborated by Belaroui et al.[17] through their work using confocal Raman spectroscopy. Proposing a general explanation for the distribution of surfactants, Kientz et al. enlisted three main factors controlling the distribution: initial surfactant distribution (amounts present at various interfaces), surfactant desorption during film drying, and the mobility of surfactants after desorption. They argued that the desorption and mobility of surfactants are in turn dependent on the polymer−surfactant interactions. This work has stressed the need to have a better understanding on polymer−surfactant interactions to fully address the surfactant distribution problem.

Though Tzitzinou et al.[18] observed surfactant enrichment at the surfaces of acrylic latex films like several other researchers, they provided a different explanation for the enrichment They suggested that surfactant present at the air−water interface adsorbs onto the particles as a drying front moves downward due to water evaporation. This surfactant deposited on the particles is reflected in their RBS measurements. Kientz et al. argues that the surface area of the air−water interface is much less compared to the particle−water interface and thus there is generally very little surfactant amount at the air−water interface.[16]

In recent years in an effort to altogether eliminate surfactant desorption during drying and annealing stages, new surfactants which permanently adsorb onto particle surfaces have been designed. Research has shown that reactive surfactants such as sodium tetradecyl maleate help reduce the exudation to the film surfaces by permanently adsorbing onto particle surfaces.[19] These surfactants seem to be good alternatives to conventional surfactants and certainly warrant further attention.

A review of the experimental work into surfactant distribution carried out so far shows that surfactant excesses or depletions have been reported at air/polymer, substrate/polymer interfaces or both depending on the systems used and the operating drying conditions. There has been intense speculation and debate on the exact parameters that influence surfactant distributions and cause nonuniformities. It is evident that modeling the surfactant transport during film drying is called for. In this paper we derive the conservation equation for surfactant transport during the water evaporation stage. The model predicts the surfactant distribution across the entire depth of a film at the end of the solvent evaporation stage. This model depends on the adsorption isotherm and surfactant diffusion only. Parametric analysis is made using the model to see the influence of the adsorption isotherm on surfactant distribution. We then compare some predictions with ATR-FTIR results for model systems.

Model

Mathematical Formulation. In arriving at the conservation equation for surfactant during the solvent evaporation stage, it was assumed that solvent evaporation occurs uniformly from the top surface. This is valid many capillary distances away from the edge,[20] thus we ignore the complication of lateral drying. The rationale for this is to split any vertical and horizontal stratifications into separate problems. Evaporation occurs at a constant rate, giving a fixed velocity E to the top air−water interface. The particle distribution across the film is determined by a dimensionless Peclet number, Pe_p given by $Pe_p = H_0E/D_p$. H_0 is the initial film thickness, and D_p is the particle diffusion coefficient. The distribution of particle volume fraction (ϕ) is given by solution of

$$\frac{\partial \phi}{\partial \bar{t}} = \frac{1}{Pe_p}\frac{\partial^2 \phi}{\partial \bar{y}^2}$$

with no flux conditions at the top and bottom. For $Pe_p \gg 1$, the air−water interface moves at a rate much faster than the particles can diffuse. This causes accumulation of particles at regions close to the air−water interface leading to a discontinuity in particle volume fraction, a phenomenon observed by several researchers.[21] In this modeling approach, we solve the surfactant conservation equation in the limit of high particle Peclet number. But it should be noted that the case of moderate particle Peclet number also deserves attention in the future. From a simple mass balance, it can be shown that the position of a particle front ($\overline{h_p}$) that separates a region of close packed volume fraction (ϕ_m) from a region with still initial particle volume fraction (ϕ_0), is given by[22]

$$\overline{h_p} = 1 - \frac{\phi_m \bar{t}}{\phi_m - \phi_0}$$

In all the simulations in this work, the initial particle volume fraction of the dispersion (ϕ_0) is taken as 0.4 and drying is carried out until the particle volume fraction reaches 0.64. This value of 0.64 for ϕ_m corresponds to the random packing volume fraction that would be obtained at the end of evaporation stage if no particle contact or deformation takes place during this stage. This is an inherent assumption of the model.

Time is scaled with a characteristic drying time (H_0/E), and dimensionless quantities are designated with an over

(13) Evanson, K. W.; Thorstenson, T. A.; Urban, M. W. *J. Appl. Polym. Sci.* **1991**, *42*, 2297.
(14) Zhao, Y.; Urban, M. W. *Macromolecules* **2000**, *33*, 2184.
(15) Zhao, Y.; Urban, M. W. *Langmuir* **2000**, *16*, 9439.
(16) Kientz, E.; Holl, Y. *Colloids Surf., A* **1993**, *78*, 255.
(17) Belaroui, F.; Hirn, M. P.; Grohens, Y.; Marie, P.; Holl, Y.; *J. Colloid Interface Sci.* **2003**, *261*, 336.
(18) Tzitzinou, P. M. Jenneson, A. S.; Clough, J. L.; Keddie, J. L.; Lu, J. R.; Zhdan, P.; Treacher, K. E.; Satguru, R. *Prog. Org. Coat.* **1999**, *35*, 89.
(19) Aramendia, E.; Mallegol, J.; Jeynes, C.; Barandiaran, M. J.; Keddie, J. L.; Asua, J. M. *Langmuir* **2003**, *19*, 3212.
(20) Routh, A. F.; Russel, W. B. *AIChE J.* **1998**, *44*, 4 (9), 2088.
(21) Croll, S. G. *J. Coat. Technol.* **1986**, *58*, 41.
(22) Routh, A. F.; Zimmerman, W. B. *Chem. Eng. Sci.* **2004**, *59*, 2961.

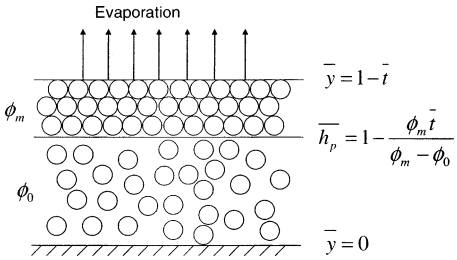

Figure 1. Schematic of a drying latex film showing the recession of the top surface and the propagation of the particle front.

bar. Distances are scaled with initial film thickness, H_0. The schematic of a propagating particle front is shown in Figure 1. This problem is considered in detail in a previous publication.[22]

The surfactant in a latex dispersion partly adsorbs onto the particles and partly remains in the bulk solution. At equilibrium, the amount that adsorbs to the particles is related to the amount in solution by an adsorption isotherm. This is typically given the symbol Γ.

The conservation equation for surfactant is written as

$$\frac{\partial(\overline{C_S}(1-\phi)+\bar{\Gamma}\phi)}{\partial \bar{t}} = \frac{1}{Pe_s}\frac{\partial\left((1-\phi)\dfrac{\partial \overline{C_S}}{\partial \bar{y}}\right)}{\partial \bar{y}} + \frac{1}{Pe_p}\frac{\partial\left(\bar{\Gamma}\dfrac{\partial \phi}{\partial \bar{y}}\right)}{\partial \bar{y}} \quad (1)$$

where $\overline{C_S}$ and $\bar{\Gamma}$ are the surfactant concentrations in bulk solution and on particles, respectively, scaled with C_{S0}, the initial surfactant concentration in the bulk ($\bar{\Gamma}$ is defined explicitly later). Pe_S is the surfactant Peclet number. For $Pe_p \gg 1$, the particle volume fraction ϕ is given by a step function, hence

$$\phi = \phi_0 + (\phi_m - \phi_0)H(\bar{y} - \overline{h_p}) \quad (2)$$

where $H(x)$ is a heaviside step function. The boundary conditions on eq 1 are no surfactant flux at the bottom (substrate) and top (moving air−film interface) boundaries.

$$\bar{y} = 0 \quad \frac{\partial \overline{C_S}}{\partial \bar{y}} = 0$$

$$\bar{y} = 1 - \bar{t} \quad (1-\phi)\frac{\partial(\overline{C_S})}{\partial \bar{y}} = Pe_S((1-\phi)\overline{C_S} + \phi\bar{\Gamma})$$

The initial condition is arbitrary and taken as a uniform surfactant concentration across the film thickness

$$\overline{C_S}(\bar{t}=0) = 1$$

To simplify the current double moving boundary problem (air−film interface and particle front) to a single moving boundary problem (particle front), a coordinate transformation is made. As the position of the top air−film interface is given by $\bar{y} = 1 - t$, defining a new vertical coordinate $\xi = \bar{y}/(1 - t)$ helps us fix the top surface. It should be noted that this change in coordinate system only helps us in better handling of the problem numerically but does not change the physics of the problem. The new vertical coordinate ξ and time τ are defined as

$$\xi = \frac{\bar{y}}{1-\bar{t}} \qquad \tau = \bar{t}$$

Substituting eq 2 into eq 1, ignoring the particle diffusion terms since we assume $Pe_p \gg 1$, and making the coordinate transformation gives the surfactant conservation equation as

$$\left(1 - \phi + \phi\frac{d\bar{\Gamma}}{d\overline{C_S}}\right)\left(\frac{\partial \overline{C_S}}{\partial \tau} + \frac{\xi}{1-\tau}\frac{\partial \overline{C_S}}{\partial \xi}\right) - \frac{1}{Pe_s(1-\tau)^2}\frac{\partial\left((1-\phi)\dfrac{\partial \overline{C_S}}{\partial \xi}\right)}{\partial \xi} + \frac{(\bar{\Gamma} - \overline{C_S})\phi_m}{(1-\tau)}\delta(\xi - \xi_p) = 0 \quad (3)$$

where $\delta(\xi - \xi_p)$ is a dirac delta function, arising from the heaviside step function used for the particle volume fraction. ξ_p represents the position of the particle front in the new coordinate system given by

$$\xi_p = \frac{1 - \left(\dfrac{\phi_m}{\phi_m - \phi_0}\right)\tau}{1-\tau} \quad (4)$$

The transformed boundary conditions and initial condition on eq 3 are

$$\xi = 0 \quad \frac{\partial \overline{C_S}}{\partial \bar{\xi}} = 0$$

$$\xi = 1 \quad (1-\phi)\frac{\partial \overline{C_S}}{\partial \bar{\xi}} = Pe_s((1-\phi)\overline{C_S} + \phi\bar{\Gamma})(1-\tau)$$

$$\overline{C_S}(\tau=0) = 1$$

Assuming the surfactant adsorption onto latex particles to be of Langmuir type, the isotherm is given by $\Gamma = \Gamma_\infty C_S/(A + C_S)$, where Γ is in mol/m^2. Hence in terms of concentration, we obtain a dimensionless isotherm $\bar{\Gamma}$ as

$$\bar{\Gamma} = \frac{\dfrac{3\Gamma_\infty}{RC_{S0}}\overline{C_S}}{\dfrac{A}{C_{S0}} + \overline{C_S}} \equiv \frac{k\overline{C_S}}{\bar{A} + \overline{C_S}} \quad (5)$$

Γ_∞ and A are Langmuir isotherm parameters, Γ_∞ representing the maximum surface adsorption onto the particles and A representing the concentration at which significant adsorption (about half the maximum surface adsorption) occurs. These parameters are constant for a given surfactant−latex system at constant temperature. The parameter k is defined as $3\Gamma_\infty/RC_{S0}$, representing the maximum surfactant adsorption onto particles scaled with respect to the initial bulk concentration C_{S0}. $\bar{A}$ is defined as A/C_{S0} and represents the critical concentrations scaled with respect to the initial bulk concentration.

Equation 3 is solved numerically for $\overline{C_S}$ using FemLab.[23] Space is discretized using a finite element method

(23) Zimmerman, W. B. *Process Modeling and Simulation with Finite Element Methods*; World Scientific: Singapore, 2003.

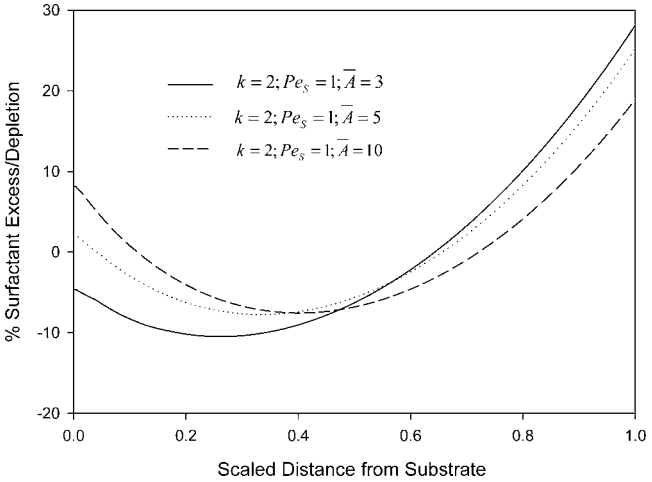

Figure 2. Percent surfactant excess/depletion at the end of drying (particle volume fraction is 0.64) as a function of scaled distance from substrate for different $\bar{A}$ values greater than 1, at fixed k and Pe_S values.

with 2000 elements. A time step of 10^{-3} is used. From the solution for $\overline{C_S}$ as a function of space and time, we obtain the total surfactant weight % across the film depth as drying proceeds.

Results and Discussion

In this section we present the results showing the influence of scaled Langmuir isotherm parameters k and $\bar{A}$, and the surfactant Peclet number Pe_S on the surfactant distribution across the film depth at the end of the water evaporation stage. The surfactant distribution is represented as % excess/depletion of surfactant over the amount that would be expected if the surfactant were uniformly distributed. This is given at any point ξ at the end of drying by

$$\frac{\left(\left(\phi_m \frac{k\overline{C_S}}{\bar{A}+\overline{C_S}} + (1-\phi_m)\overline{C_S}\right)(1-\tau) - \left(\phi_0 \frac{k\overline{C_S}}{\bar{A}+\overline{C_S}} + (1-\phi_0)\overline{C_S}\right)\Big|_{\bar{t}=0}\right) \times 100}{\left(\phi_0 \frac{k\overline{C_S}}{\bar{A}+\overline{C_S}} + (1-\phi_0)\overline{C_S}\right)\Big|_{\bar{t}=0}}$$

Figure 2 shows the influence of $\bar{A}$ on surfactant distribution profiles for fixed k and Pe_S values. It can be seen that there is an excess of surfactant in the upper region of the film for all three values of $\bar{A}$. Throughout the drying process, the upper regions of the film have higher particle volume fractions compared to the lower regions of the film. As drying proceeds, the surfactant concentration increases in the bulk due to water evaporation, and as a result, there is more adsorption onto the particles. As a result of the increasing particle volume fraction and increasing adsorption onto particles, the upper regions of the film grow laden with surfactant which is reflected in the three curves.

As the value of $\bar{A}$ increases from 3 to 10, there is a decrease in the % excess that is seen closer to the film−air interface. If the value of $\bar{A}$ is high enough, a surfactant excess can also been seen toward the substrate side of the film. A higher $\bar{A}$ value indicates less adsorption of surfactant onto the particles. If this is low, lower regions of the film, where the water content is high, can have higher concentrations of surfactant, as can be seen in the case of $\bar{A} = 5$ and $\bar{A} = 10$. For $\bar{A} = 3$, desorption into solution is not high enough to show any excess surfactant at the film−substrate interface.

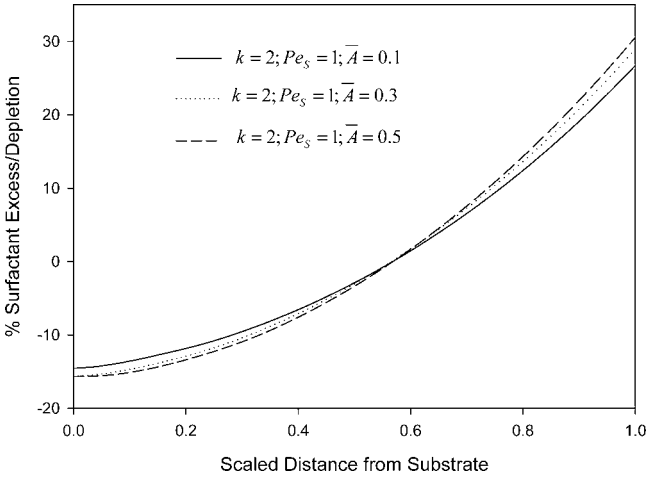

Figure 3. Percent surfactant excess/depletion at the end of drying (particle volume fraction is 0.64) as a function of scaled distance from substrate for different $\bar{A}$ values less than 1, at fixed k and Pe_S values.

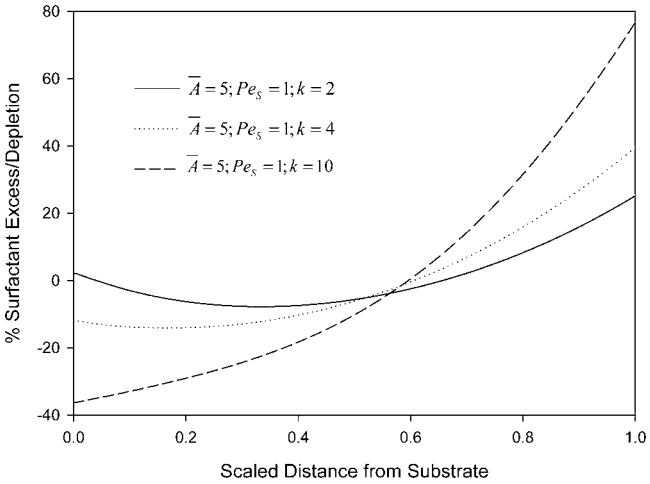

Figure 4. Percent surfactant excess/depletion at the end of drying (particle volume fraction is 0.64) as a function of scaled distance from substrate for different k values, at fixed $\bar{A}$ and Pe_S values.

Figure 3 shows the distribution profiles for fixed k and Pe_S values, but for $\bar{A}$ values less than 1. These values of $\bar{A}$ correspond to the flat region of the Langmuir isotherm, where the particles are saturated with surfactant and there is little exchange taking place. As expected, there is excess of surfactant in the upper region of the film for all values of $\bar{A}$. In addition, there is always a depletion toward the substrate side of the film because there is a depletion of surfactant in the water phase. The interesting observation is that, in contrast to the behavior shown in Figure 2, increasing the $\bar{A}$ value from 0.1 to 0.5 results in an increase in percent excess seen at the air−film interface. Increasing $\bar{A}$ values from 0.1 to 0.5 corresponds to lowering the surfactant concentration in the bulk without much change in the concentration on the particles. As a result, the surfactant content in the lower region of the film (which has higher water content) is lower for higher values of $\bar{A}$ and thus shows greater depletion. This greater surfactant depletion in the lower region is reflected in the greater surfactant excess seen in the upper portions of the film for higher values of $\bar{A}$.

Figure 4 shows the influence of particle surfactant saturation limit, parameter k, on surfactant distribution profiles, at fixed $\bar{A}$ and Pe_S values. For all three values of k, the upper portion of the film has excess surfactant,

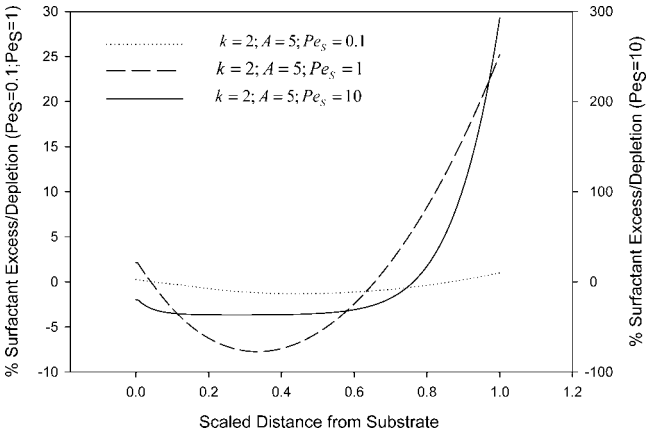

Figure 5. Percent surfactant excess/depletion at the end of drying (particle volume fraction is 0.64) as a function of scaled distance from substrate at different Pe_S values, for fixed isotherm.

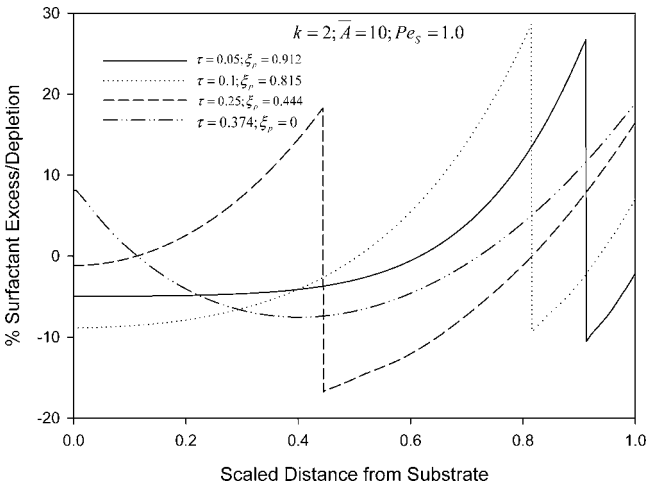

Figure 6. Percent surfactant excess/depletion at different stages of drying as a function of scaled distance from substrate for fixed k, $\bar{A}$, and Pe_S values (τ is time and ξ_p is position of particle front).

with the percent excess increasing with increasing k value. Higher values of k indicate higher surfactant amounts on particles for a given amount of surfactant in the latex dispersion. A higher surfactant amount on particles means higher surfactant amounts in the upper regions of the film where the particle volume fraction is higher throughout the drying stage.

The influence of surfactant Peclet number, Pe_S, on surfactant distribution profiles for given set of Langmuir parameters is shown in Figure 5. For sufficiently low Peclet number ($Pe_S = 0.1$), the surfactant diffusion through water is high enough that the surfactant distribution profile is almost uniform through the entire thickness of the film. With increasing Peclet number, the nonuniformity in surfactant distribution increases, with the excess surfactant reaching high proportions for $Pe_S = 10$. For high Peclet number, the surfactant diffusion is so low that there is huge accumulation toward the film−air interface and a major region of the film is depleted in surfactant.

Finally, surfactant distribution profiles at different stages during the drying process are also plotted (Figure 6) to show the evolution of surfactant distribution with time for a given set of k, $\bar{A}$, and Pe_S values. During solvent evaporation, the particle front (vertical lines in the curves) moves from the film−air interface toward the substrate. The four curves represent the surfactant distribution profiles for four different times. It can be noted that during the solvent evaporation stage the surfactant distribution profiles are not continuous across the entire film thickness but have a discontinuity at the particle front position. This discontinuity is due to the sharp change in particle volume fraction at the particle front position. When the particle volume fraction is finally uniform ($\tau = 0.374$; $\xi_p = 0$), the surfactant profile is a continuous curve.

From this theoretical analysis, we are able to show that the Langmuir isotherm parameters and surfactant Peclet number are controlling the surfactant distribution profiles obtained at the end of the solvent evaporation stage. In all the cases studied, the upper portions of the films are laden with excess surfactant, with the amount in excess dependent on the magnitudes of k, $\bar{A}$, and Pe_S values. If the value of $\bar{A}$ is sufficiently high, excess can be seen even near the film−substrate interface. In practice, the Langmuir isotherm parameters are dependent on the surfactant−latex systems used. Due to the manner in which we have scaled k and $\bar{A}$, the surfactant distribution profiles are also influenced by the initial surfactant amount in solution. The Peclet number Pe_S depends on the type of surfactant used, thickness of the film, and drying rate. With the right system chosen and by the drying conditions controlled, nonuniformities in surfactant distribution can be controlled. In the next section, we provide experimental verification to the model predictions and show the limitations of the model and experimental surfactant measuring procedures.

Materials and Methods

Latex Preparation. The latices used in these experiments were 50/50 mixtures by weight of styrene and butyl acrylate monomers. They were made surfactant free via emulsion polymerization[24] using 2-methyl propionamidine as the initiator. The reaction was carried out in a glass reactor equipped with a reflux condenser, glass stirrer at 300 rpm, nitrogen inlet, and water jacket to maintain the reaction temperature at 70 °C. The butyl acrylate monomer (Argos Organics) was vacuum distilled and styrene monomer (Argos Organics) passed through aluminum oxide to remove the inhibitors. The polymerization is carried in a semicontinuous process. Water was added to the reactor, and the reactor is heated and purged with nitrogen. Half of the monomer mixture was added into the reactor. The next step involved addition of the initiator, followed by addition of the rest of the monomers over a period of 3−4 h. The reaction was allowed to proceed overnight to ensure complete conversion. The latex produced was cleaned by dialysis for a week to remove impurities and unreacted reagents. The mean particle sizes were measured by dynamic light scattering (Brookhaven Zeta Plus). The particles formed a coherent film when dried at room temperature.

Surfactant Adsorption Isotherms. Cationic surfactant cetyltrimethylammonium bromide (CTAB) (Sigma-Aldrich, used as received) and nonionic surfactant Triton X-100 (Sigma-Aldrich, used as received) were used in these experiments. The adsorption isotherms for the two surfactants were obtained by a solution depletion method. In this method, known amounts of surfactants were added to known weights of latex and the samples were shaken for several hours and left overnight to equilibrate. They were then centrifuged using a Micro Centaur centrifuge at 13000 rpm. The supernatants for the two surfactants were treated and analyzed in separate ways to measure the surfactant concentrations. For the supernatant containing CTAB, a solution of the supernatant was prepared in 40 mL of water and 1 mL of 0.1% picric acid in 0.002 M NaOH was added. It was then shaken with 20 mL of redistilled 1,2-dichloroethane and centrifuged, and the UV-absorbance of the organic phase was measured at 375 nm using a Helios UV−vis spectrometer.[25] For the supernatant containing Triton, a constant pH was maintained by adding

(24) Vanderhoff, J. W. *J. Polym. Sci., Polym. Symp.* **1985**, *72*, 161.
(25) Rosen, M. J.; Goldsmith, H. A. *Systematic Analysis of Surface-Active Agents*; Wiley-Interscience: New York, 1972.

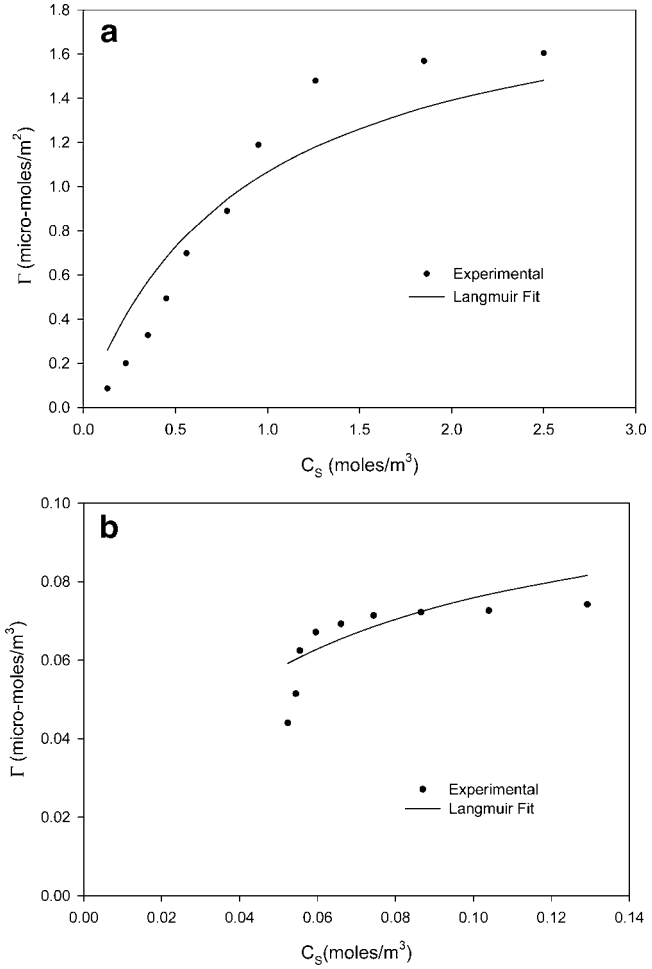

Figure 7. (a) Adsorption isotherm for cationic surfactant HTAB on styrene−butyl acrylate copolymer latex particles. (b) Adsorption isotherm for nonionic surfactant Triton X-100 on styrene−butyl acrylate copolymer latex particles.

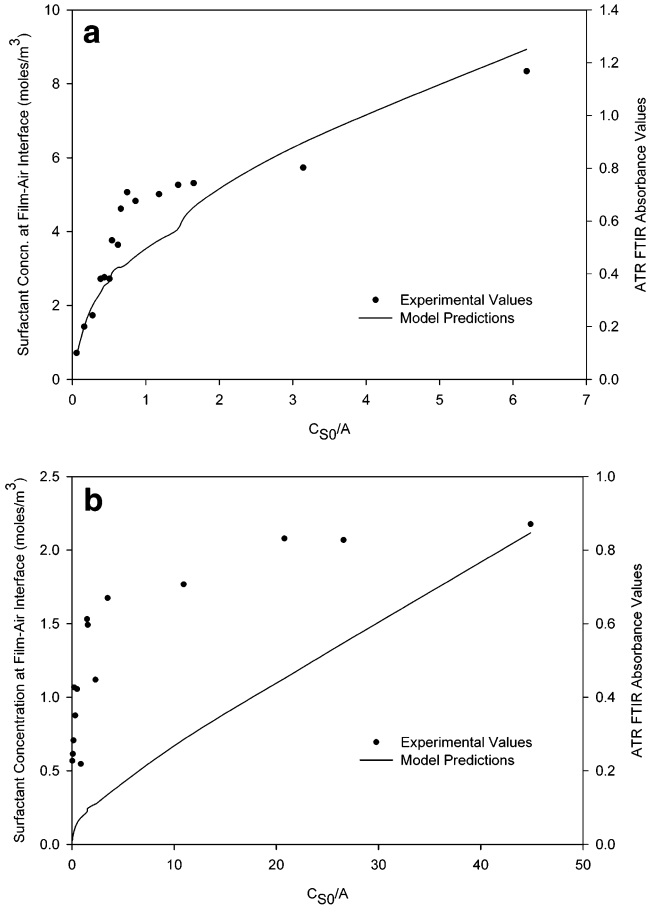

Figure 8. (a) Surfactant concentrations and ATR absorbance values at the film−air interface as functions of critical surfactant bulk concentrations for CTAB. (b) Surfactant concentrations and ATR absorbance values at the film−air interface as functions of critical surfactant bulk concentrations for Triton X-100.

phosphate-buffered saline to the supernatant. The surfactant concentration in the supernatant was then obtained by measuring the UV absorbance at 276 nm using an Ultrospec 2100 Pro UV−vis spectrometer. The amount of surfactant present in solution when subtracted from the initial surfactant amount added to the latex sample gives the amount adsorbed onto the particles. A plot of surfactant amount adsorbed onto particles (expressed in moles/m^2) vs the surfactant concentration in the bulk (expressed in moles/m^3) gives the adsorption isotherm for the surfactants.

ATR FTIR Spectroscopy. Surfactants were added to known amounts of latex in varying proportions to obtain latex samples with different surfactant weight percents. For the samples containing CTAB surfactant, the surfactant weight percent with respect to polymer was varied from 0.2% to 10%. For the samples containing Triton surfactant, the surfactant weight percent with respect to polymer was varied from 0.01% to 2%. The samples were thoroughly shaken and allowed to equilibrate overnight. The samples were then cast onto aluminum foils and dried for a day. The air−film interfaces of the dried films were probed for surfactant presence using ATR-FTIR spectroscopy. The instrument used was a Perkin-Elmer Spectrum One FTIR spectrometer. The spectrometer was used in point and reflectance mode.

Results and Discussion

The particle diameters were 196 nm. Parts a and b of Figure 7 show the adsorption isotherms for CTAB and Triton X-100, respectively. The bulk concentration at which particle saturation occurs is much lower for Triton compared to CTAB because of its lower solubility in water. The data from the two isotherms were fit with Langmuir-type isotherms to obtain the Langmuir parameters Γ_∞ and A (eq 5). From Figure 7, it is evident that a Langmuir fit is not an ideal fit for the data obtained. This shows that it is not a simple Langmuir adsorption which takes place, but a more complicated adsorption process. In addition to the hydrophobic interactions between the surfactant species and the particle surface, there may be mutual interactions between the adsorbed species which are not accounted by the Langmuir model. As there is no proper alternate adsorption mechanism at present, we use the best Langmuir fit to the data for our analysis. The values obtained for these parameters for the two surfactants are shown in Table 1. These values along with the initial bulk concentrations C_{S0}, for each latex sample, give the scaled Langmuir parameters k and $\bar{A}$. Using a value of 0.3 cm/day for E,[26] 1 mm for H_0, and a surfactant diffusion coefficient value of 4×10^{-10} m^2/s, we estimate the surfactant Peclet number Pe_S to be 0.1. These scaled parameters were put into the model to obtain a prediction for the surfactant concentration at the film−air interface at the end of drying. We estimate the particle Peclet

Table 1. Langmuir Parameters Fitted from the Isotherm for the Surfactants

surfactant	Γ_∞ (μmol/m^2)	A (mol/m^3)
CTAB	2.0	0.875
Triton X-100	0.11	0.045

(26) Keddie, J. L.; Meredith, P.; Jones, R. A. L.; Donald, A. M. *Macromolecules* **1995**, *28*, 1673.

number to be 20, which gives a close approximation to a step function for the particle profile.[22]

It should be noted that here we obtain the surfactant concentrations from the model using a final particle volume fraction of 0.64 (end of solvent evaporation stage) and compare them with experimentally determined surface concentrations in films which have dried further. To do this, we assume that the surfactant distribution is well established during the evaporation stage and evolves very little thereafter.[17] Even though desorption occurs during the later stages due to deformation and coalescence, the transport taking place is considerably smaller than when water is present and hence surfactant concentrations remain similar to their values at the end of the evaporation stage.

The characteristic bands chosen for the two surfactants were the 1030 cm^{-1} band for CTAB, corresponding to the C−N stretching bond and the 1065 cm^{-1} band for Triton, corresponding to the C−O stretching bond. Parts a and b of Figure 8 show the plots of surfactant concentration at the film−air interface predicted by the model and ATR absorbance values, as functions of a scaled parameter C_{S0}/A, for CTAB and Triton, respectively. The parameter C_{S0}/A determines the region of the isotherm over which the adsorption desorption phenomena takes place for a given latex sample during drying. Values of $C_{S0}/A \gg 1$ correspond to the flat region of the Langmuir isotherm, where the particles are saturated with surfactant and there is little exchange taking place. The absorbance values from ATR-FTIR spectroscopic analysis indicate two regions with different slopes with a transition around $C_{S0}/A = 1$ for both surfactants. This scaling argument shows the adsorption isotherm to be controlling. As can be seen, in the case of both surfactants the model also predicts two regions of surfactant distribution behavior. For values of $C_{S0}/A < 1$, there is a steeper increase in the surfactant concentration with increasing C_{S0}/A values. This is due to the greater adsorption/desorption taking place in this region. It should be noted here that though the experimental results conform to the behavior predicted by the model, direct comparison is difficult as there is no standard way of interpreting absorbance values in terms of surfactant concentrations. Also it is evident that the agreement between the experimental and modeling values for Triton surface concentration is poor in comparison to CTAB. This is due to the poorer Langmuir fit for Triton compared to CTAB. However from this qualitative analysis using the model and ATR-FTIR spectroscopy, we were able to show that the model correctly predicts that the surfactant concentrations obtained at the film−air interface are dependent on the adsorption isotherm.

Conclusions

These studies show that an adsorption isotherm and surfactant diffusion are the determining physical parameters for surfactant distributions in latex films. Surfactant excesses at the top surface are always predicted by the model. The magnitudes of the isotherm parameters determine whether surfactant excesses or depletions are predicted at the substrate. Uniform distributions are obtained when the surfactant Peclet number is low. The ATR-FTIR results conform qualitatively to the model predictions on the dependence of interfacial surfactant concentrations on the adsorption isotherm.

Acknowledgment. This work is financially supported by EPSRC through Grant GR/S05885/01. The authors are grateful to Peter Styring for help with FTIR.

LA048939B